AMERICAN ACADEMY OF OPHTHALMOLOGY®

# Spectral-Domain and Swept-Source OCT Angiographic Scans Yield Similar Drusen Measurements When Processed with the Same Algorithm

*Farhan E. Hiya, MD,[1] Jeremy Y. Liu, MD,[1] Mengxi Shen, MD,[1] Gissel Herrera, MD,[1] Jianqing Li, MD,[1,2] Qinqin Zhang, PhD,[3] Luis de Sisternes, PhD,[3] Robert C. O'Brien, PhD,[1] Philip J. Rosenfeld, PhD, MD,[1] Giovanni Gregori, PhD[1]*

***Purpose:*** An algorithm developed to obtain drusen area and volume measurements using swept-source OCT angiography (SS-OCTA) scans was tested on spectral-domain OCT angiography (SD-OCTA) scans.

***Design:*** Retrospective study.

***Participants:*** Forty pairs of scans from 27 eyes with intermediate age-related macular degeneration and drusen.

***Methods:*** Patients underwent both SD-OCTA and SS-OCTA imaging at the same visit using the 6 mm × 6 mm OCTA scan patterns. Using the same algorithm, we obtained drusen area and volume measurements within both 3 mm and 5 mm fovea-centered circles. Paired 2-sample *t*-tests were performed along with Pearson's correlation tests.

***Main Outcome Measures:*** Mean square root (sqrt) drusen area and cube root (cbrt) drusen volume within the 3 mm and 5 mm fovea-centered circles.

***Results:*** Mean sqrt drusen area values from SD-OCTA and SS-OCTA scans were 1.57 (standard deviation [SD] 0.57) mm and 1.49 (SD 0.58) mm in the 3 mm circle and 1.88 (SD 0.59) mm and 1.76 (SD 0.58) mm in the 5 mm circle, respectively. Mean cbrt drusen volume measurements were 0.54 (SD 0.19) mm and 0.51 (SD 0.20) mm in the 3 mm circle, and 0.60 (SD 0.17) mm and 0.57 (SD 0.17) mm in the 5 mm circle. Small differences in area and volume measurements were found (all $P < 0.001$); however, the correlations between the instruments were strong (all coefficients $> 0.97$; all $P < 0.001$).

***Conclusions:*** An algorithm originally developed for SS-OCTA scans performs well when used to obtain drusen volume and area measurements from SD-OCTA scans; thus, a separate SD-OCT structural scan is unnecessary to obtain measurements of drusen.

***Financial Disclosure(s):*** Proprietary or commercial disclosure may be found in the Footnotes and Disclosures at the end of this article. *Ophthalmology Science 2024;4:100424 © 2024 Published by Elsevier Inc. on behalf of the American Academy of Ophthalmology. This is an open access article under the CC BY-NC-ND license (http://creativecommons.org/licenses/by-nc-nd/4.0/).*

Age-related macular degeneration (AMD) is a complex genetic disease and a leading cause of irreversible vision loss among the elderly worldwide.[1] Age-related macular degeneration is currently classified into 3 clinical stages: early, intermediate, and late.[1,2] Early and intermediate AMD (iAMD) are distinguished based on the size of drusen, with iAMD also defined by the presence of pigmentary changes.[1,2] Late AMD is defined by the presence of exudative macular neovascularization or geographic atrophy, also known as complete retinal pigment epithelium (RPE) and outer retinal atrophy.[1–3] Historically, the area occupied by drusen, which are lipoprotein deposits located between Bruch's membrane (BM) and the RPE, has been measured using color fundus imaging; however, reproducible drusen area and volume measurements can be obtained from OCT datasets using algorithms capable of segmenting the RPE and BM.[4–11] These drusen volume measurements, along with other anatomic parameters such as the presence of hyper-reflective foci, calcified drusen, and reticular pseudodrusen, have been used to help identify eyes at high-risk for disease progression from iAMD to late AMD.[1,2,7,8,12–17]

Recently, a new, highly reproducible algorithm, the Advanced RPE Analysis v0.10 (ARA10), was developed to measure drusen area and volume in eyes with iAMD from dense swept-source OCT angiography (SS-OCTA) scans.[10] We showed that drusen measurements obtained from SS-OCTA scans with the ARA10 algorithm were highly correlated with measurements obtained using a United States Food and Drug Administration-approved segmentation algorithm that has been commercially available on the Cirrus spectral-domain OCT angiography (SD-OCTA) instrument (Carl Zeiss, Meditec Inc). The ARA10 algorithm was shown to be more anatomically accurate than the SD-



https://doi.org/10.1016/j.xops.2023.100424
ISSN 2666-9145/23

OCT algorithm due to an improved BM segmentation.[10] It should be noted that the BM segmentation used in the ARA10 algorithm relied on the angiographic information in the SS-OCTA scans and cannot be used with standard OCT structural scans.[10,18]

Since SD-OCTA instruments are more widely available than SS-OCTA ones, the ARA10 algorithm would have greater clinical use if it could be used on SD-OCTA scans as well. Moreover, the ability of using a single SD-OCTA scan to provide both structural and angiographic quantitative information would remove the need for acquiring separate scans. In this report, we used the ARA10 algorithm on a set of SD-OCTA and SS-OCTA scans obtained from the same patient on the same day to evaluate its performance on the SD-OCTA scans and compare the drusen area and volume measurements to those obtained on SS-OCTA scans.

## Methods

Patients with AMD were enrolled in an ongoing prospective, observational, SS-OCT imaging study at the Bascom Palmer Eye Institute. The institutional review board of the University of Miami Miller School of Medicine approved the study and all patients signed an informed consent for this prospective SS-OCT study. The study was performed in accordance with the tenets of the Declaration of Helsinki and complied with the Health Insurance Portability and Accountability Act of 1996.

A retrospective review of enrolled subjects was performed to identify iAMD eyes with drusen imaged using 6 × 6 mm scan patterns centered on the fovea with both SS-OCTA (PLEX Elite 9000, Carl Zeiss Meditec, Inc) and SD-OCTA (Cirrus HD-OCT, Carl Zeiss Meditec, Inc) instruments at the same visit. The SD-OCTA instrument uses a central wavelength of 840 nm and a scan rate of 68 000 A-scans/second. The 6 × 6 mm SD-OCTA scan pattern consists of 350 A-scans per B-scan and 350 B-scans with each B-scan repeated twice within the macular cube protocol, resulting in a uniform 17 μm spacing between A-scans. The SS-OCTA instrument uses a central wavelength of 1050 nm and a scan rate of 100 000 A-scans/second. The 6 × 6 mm SS-OCTA scan pattern consists of 500 A-scans per B-scan and 500 B-scans with each B-scan repeated twice within the macular cube protocol, resulting in a uniform 12 μm spacing between A-scans. Both instruments have a full width at half maximum axial resolution of ~5 μm in tissue and an estimated transverse resolution of ~20 μm at the retinal surface.

Eyes were excluded if any other retinal pathologies were present, such as diabetic retinopathy, retinal vein occlusion, central serous chorioretinopathy, and late stage AMD. Scans were also excluded if they had signal strength < 7 based on the instrument's output or if they presented significant motion artifacts.

Scans were downloaded in a native export format from their respective instruments and processed using a stand-alone executable version of the ARA10, which is currently available on the PLEX Elite 9000 software (version 2.1), and was used in the study by Jiang et al.[10] For both the SD-OCTA and SS-OCTA scans, the algorithm automatically determined the foveal position within the scans, identified both a 3 mm and a 5 mm circle centered at the fovea, provided drusen area and volume measurements within the whole scan and within these predefined circles, and produced a drusen elevation map.

The square root (sqrt) transformation of the drusen area and cube root (cbrt) transformation of the drusen volume were performed to eliminate any dependence of the standard deviation (SD) of the test-retest reliability measurements on lesion size.[7,9,10] The means and SDs for drusen area and volume measurements were calculated from both scan protocols within the 3 mm and 5 mm circles centered at the fovea. The Pearson's correlation test was performed to determine the correlation between pairs of drusen area and volume measurements from the 2 imaging modalities. The paired 2-sample *t*-tests were used to compare the means of the sqrt drusen area measurements and the cbrt drusen volume measurements between SD-OCTA and SS-OCTA scans. *P* values < 0.05 were used to assess statistical significance. All statistical analysis was performed using IBM SPSS Statistics Premium for Windows, version 28.0 (IBM Corporation, Armonk, NY).

## Results

This study included a total of 40 pairs of images from 27 eyes of 22 subjects. Subjects underwent both SD-OCTA and SS-OCTA imaging on the same day between April 2021 and August 2022. Subjects were aged 55.7 to 87.8 years (mean

Table 1. Comparison of Drusen Area and Volume Measurements between Spectral-domain OCT Angiography and Swept-source OCT Angiography Scans

| | Square Root Area (3 mm Circle) | Square Root Area (5 mm Circle) | Cube Root Volume (3 mm Circle) | Cube Root Volume (5 mm Circle) |
|---|---|---|---|---|
| | Mean (SD) (mm) | Mean (SD) (mm) | Mean (SD) (mm) | Mean (SD) (mm) |
| SD-OCTA | 1.57 (0.57) | 1.88 (0.59) | 0.54 (0.19) | 0.60 (0.17) |
| SS-OCTA | 1.49 (0.58) | 1.76 (0.58) | 0.51 (0.20) | 0.57 (0.17) |
| Mean Difference 95% CI | (0.05, 0.13) | (0.06, 0.17) | (0.02, 0.04) | (0.02, 0.04) |
| *P* value | < 0.001 | < 0.001 | < 0.001 | < 0.001 |
| Regression Equations | y = 0.969x + 0.132 | y = 1.002x + 0.111 | y = 0.970x + 0.041 | y = 0.989x + 0.034 |
| Slope 95% CI | (0.91, 1.03) | (0.88, 1.12) | (0.93, 1.01) | (0.92, 1.06) |

Means and standard deviations (SDs) of square root drusen area and cube root drusen volume within the 3 mm and 5 mm circles on both spectral-domain OCT angiography (SD-OCTA) and swept-source OCT angiography (SS-OCTA) scans are presented above. *P* values for the mean differences of drusen measurements between SD-OCTA and SS-OCTA scans and the associated 95% confidence intervals (CIs) show that the differences, although small, are statistically significant. Finally, regression equations for drusen area and volume of the scan patterns are shown, along with the 95% CIs of the regression slopes. For the regression equations, x = "the drusen value obtained from a SS-OCTA scan," and y = "the drusen value obtained from a SD-OCTA scan." In all settings SD-OCTA drusen values are slightly larger than SS-OCTA measurements, while the slopes are not significantly different from one.

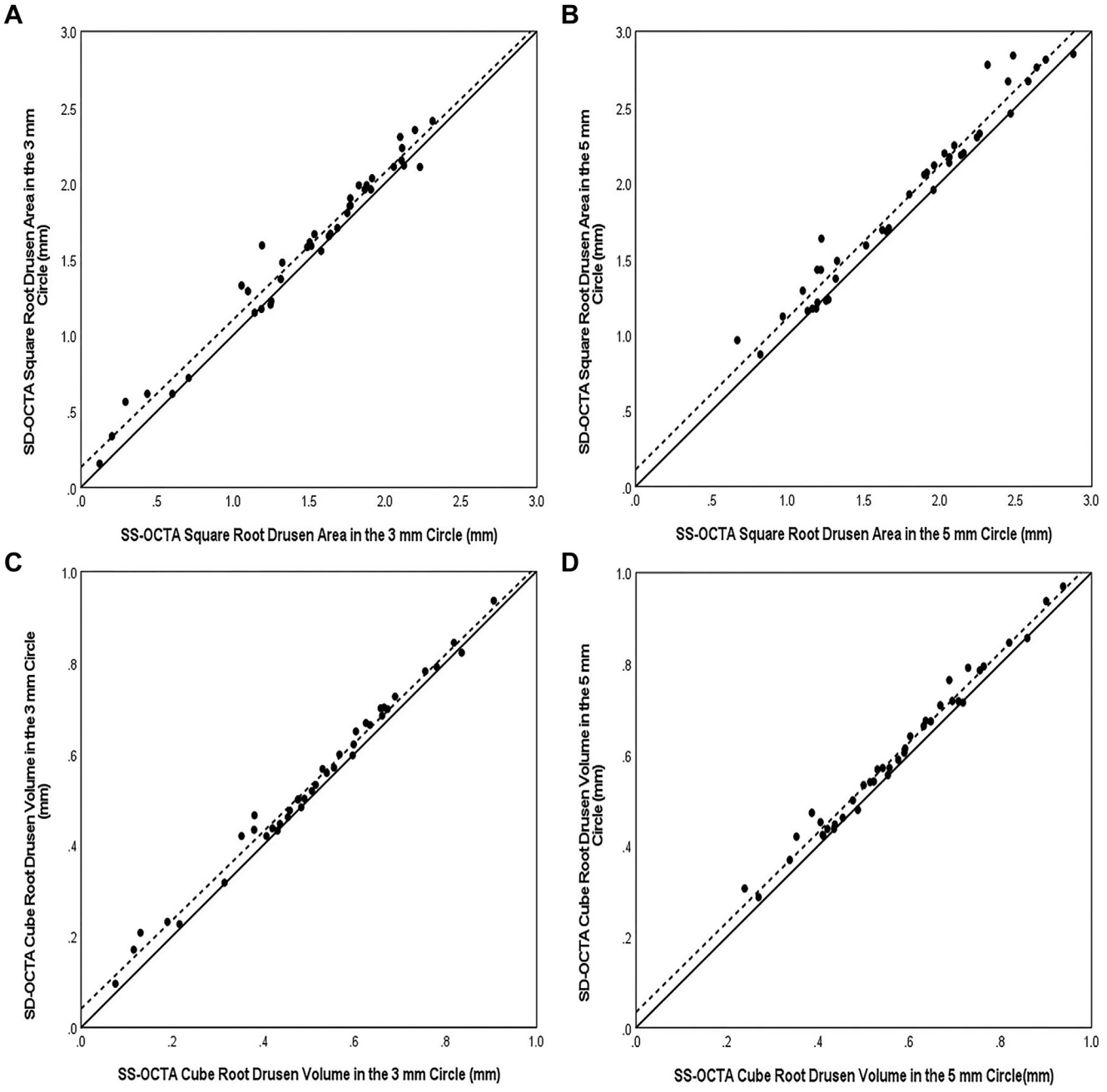


**Figure 1.** Correlation of drusen area and volume measurements between spectral-domain OCT angiographic (SD-OCTA) and swept-source OCT angiographic (SS-OCTA) scans. **A,** Square root (sqrt) drusen area in the 3 mm circle, r = 0.986. **B,** Sqrt drusen area in the 5 mm circle, r = 0.980. **C,** Cube root (cbrt) drusen volume in the 3 mm circle, r = 0.994. **D,** Cbrt drusen volume in the 5 mm circle, r = 0.992. Solid lines are lines of unity (slope = 1). Dotted lines are data regression lines. In all plots, SD-OCTA drusen values are slightly larger than, but highly correlated with, SS-OCTA measurements.

74.9, SD 6.0 years) and 59% were women. Thirteen eyes had images from 2 visits included in the study with an interval between the visits of $\geq$ 6 months (considered a clinically significant interval). Drusen area and volume measurements are described in Table 1 and Figure 1.

The mean sqrt drusen area values from SD-OCTA and SS-OCTA scans were 1.57 (SD 0.57) mm and 1.49 (SD 0.58) mm in the 3 mm circle, and 1.88 (SD 0.59) mm and 1.76 (SD 0.58) mm in the 5 mm circle, respectively. Mean cbrt drusen volume measurements were 0.54 (SD 0.19) mm and 0.51 (SD 0.20) mm in the 3 mm circle, and 0.60 (SD 0.17) mm and 0.57 (SD 0.17) mm in the 5 mm circle. The 95% confidence intervals of the mean difference between the scans are 0.05 to 0.17 mm for drusen area and 0.02 to 0.04 mm for drusen volume. Drusen area and volume measurements for the SD-OCTA scans were overall slightly

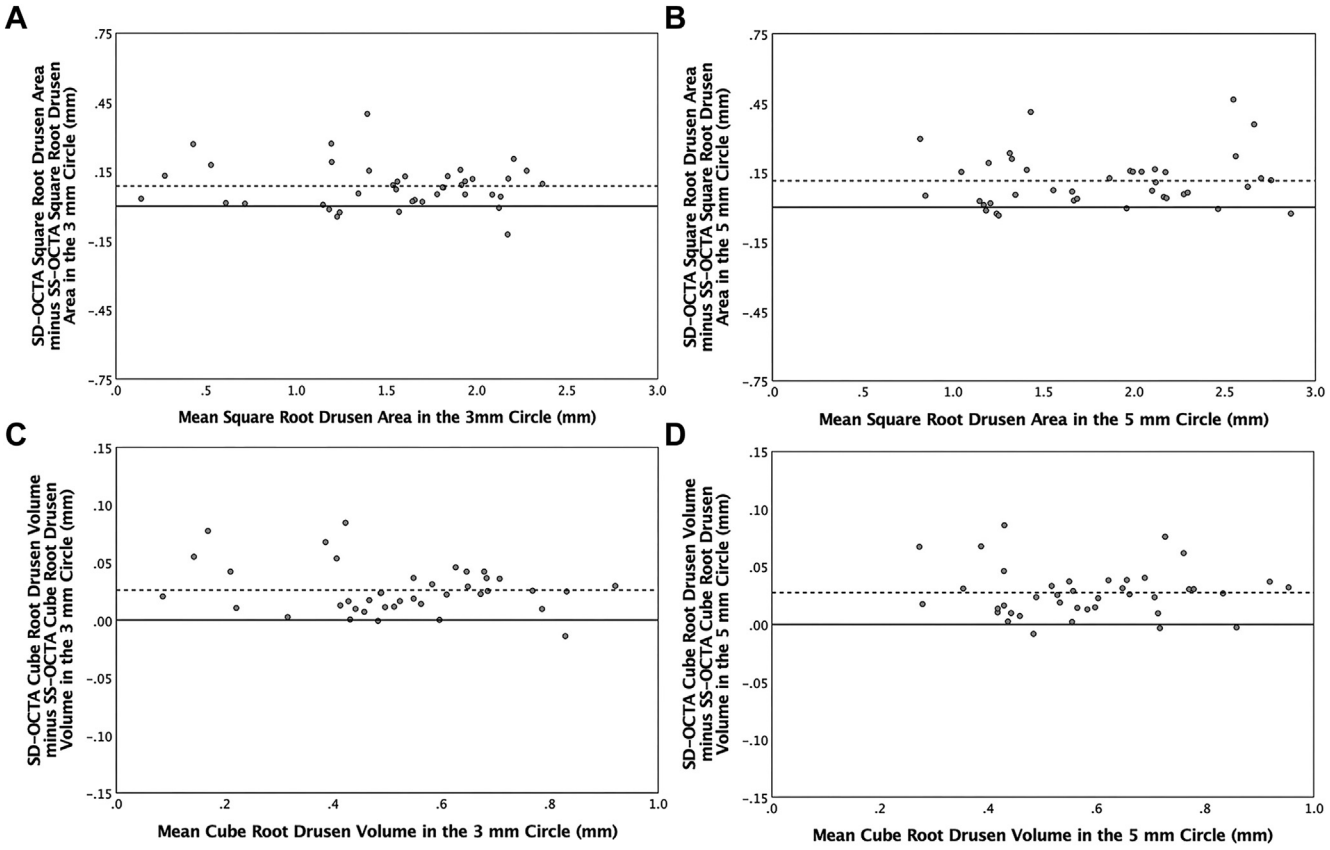


**Figure 2.** Bland-Altman plots of square root (sqrt) drusen area and cube root (cbrt) drusen volume measurements in the 3 mm and 5 mm fovea-centered circles obtained from spectral-domain OCT angiographic (SD-OCTA) and swept-source OCT angiographic (SS-OCTA) scans. **A,** Sqrt drusen area in the 3 mm circle. **B,** Sqrt drusen area in the 5 mm circle. **C,** Cbrt drusen volume in the 3 mm circle. **D,** Cbrt drusen volume in the 5 mm circle. These plots show a small systemic difference that is independent of drusen burden between the instruments, with the SD-OCTA measurements larger than the SS-OCTA measurements.

larger than those for the SS-OCTA scans and these differences were statistically significant in all cases (Table 1).

The correlations between SS-OCTA and SD-OCTA measurements were very strong and statistically significant in all cases ($P < 0.001$). The correlation coefficients were 0.986 and 0.980 for the sqrt drusen area in the 3 mm and 5 mm circles, respectively, and the correlation coefficients were 0.994 and 0.992 for the cbrt drusen volume measurements in the 3 mm circles and the 5 mm circles, respectively. Scatter plots of each of the 4 paired drusen measurements (Fig 1) and Bland-Altman plots (Fig 2) clearly show their high correlation, as well as a small average difference between the instruments, with the SD-OCTA measurements typically larger than the SS-OCTA measurements. This difference is independent of the drusen burden.

## Discussion

In this study we show that a single algorithm originally designed and validated for the quantitation of drusen area and volume measurements using SS-OCTA scans performs well on SD-OCTA scans and that structural information typically obtained using SD-OCT scans, such as drusen measurements, can be reliably obtained from SD-OCTA scans, relieving the need to acquire 2 separate scans, 1 for structural information and another for angiographic information. Moreover, it should be noted that (on the Cirrus instrument) SD-OCTA scans consist of 350 × 350 A-scans with an overall more uniform and denser sampling grid than the SD-OCT scans (either macular cube 512 × 128 or 200 × 200). In theory, these differences could allow the SD-OCTA scans to produce more detailed structural measurements than the SD-OCT scan patterns.

When using the ARA10 drusen algorithm, we found that the SD-OCTA scans produced drusen maps essentially identical to those obtained from SS-OCTA scans of the same eye. However, the drusen measurements, while highly correlated, were on average slightly larger in SD-OCTA scans and this difference was statistically significant. Figure 3 shows the drusen elevation maps of 4 representative eyes with varying drusen burdens. In these eyes, the difference between the measurements for the 2 modalities ranges between 0.11 mm and 0.36 mm for sqrt drusen area and 0.02 mm and 0.06 mm for cbrt drusen volume while little-to-no qualitative differences are noticed between the drusen maps. It is worth emphasizing

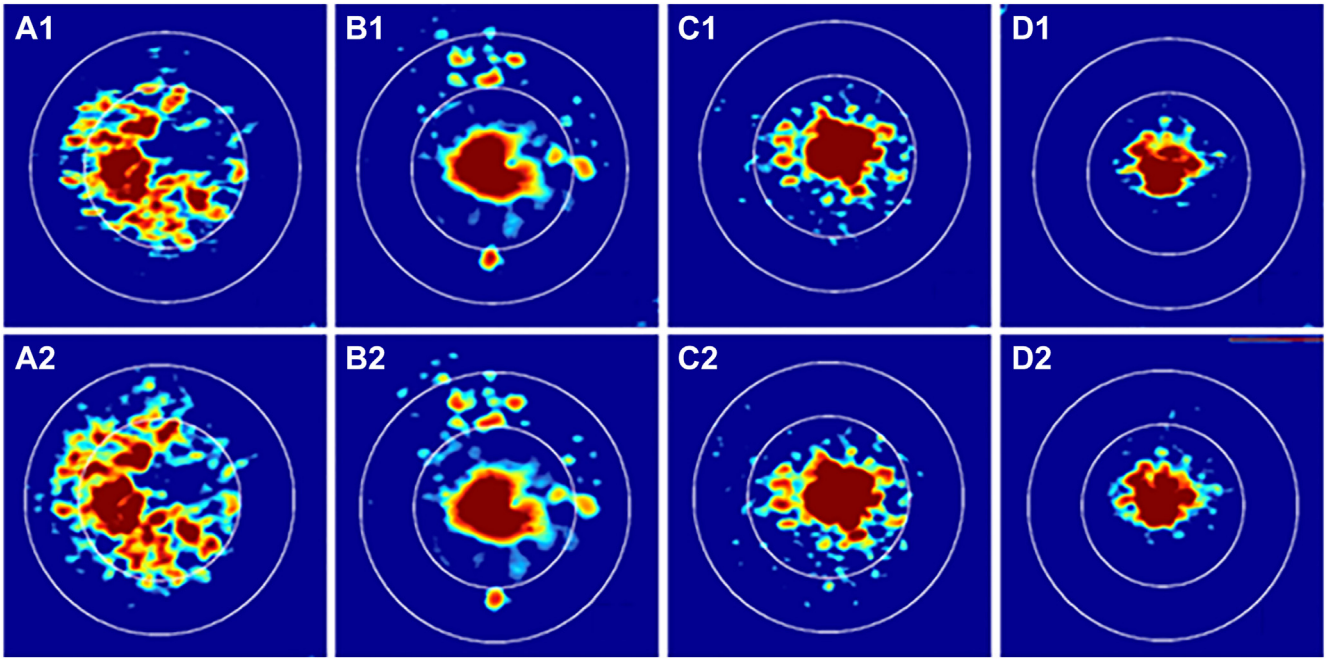


**Figure 3.** Drusen elevation maps generated by the algorithm showing comparable results in the 3 mm and 5 mm fovea-centered circles obtained from 4 cases (**A**–**D**), with a range of drusen burden, imaged at the same visit using swept-source OCT angiographic (SS-OCTA) scans (**A1, B1, C1, D1**) and spectral-domain OCT angiographic (SD-OCTA) scans (**A2, B2, C2, D2**). From the SS-OCTA and SD-OCTA scans, respectively, drusen area in the 3 mm circles were 2.20 mm and 2.35 mm (Case A), 1.77 mm and 1.90 mm (Case B), 1.88 mm and 1.99 mm (Case C), and 1.32 mm and 1.48 mm (Case D) while drusen area in the 5 mm circles were 2.48 mm and 2.84 mm (Case A), 2.10 mm and 2.25 mm (Case B), 1.91 mm and 2.07 mm (Case C), and 1.32 mm and 1.49 mm (Case D). Similarly, from the SS-OCTA and SD-OCTA scans, respectively, drusen volume in the 3 mm circles were 0.69 mm and 0.73 mm (Case A), 0.60 mm and 0.62 mm (Case B), 0.67 mm and 0.70 mm (Case C), and 0.53 mm and 0.57 mm (Case D) while drusen volume in the 5 mm circles were 0.73 mm and 0.79 mm (Case A), 0.65 mm and 0.67 mm (Case B), 0.67 mm and 0.71 mm (Case C), and 0.53 mm and 0.57 mm (Case D). The patterns of drusen elevation show only minor qualitative differences between the 2 modalities.

that the small average difference between 2 measurements, while statistically significant, essentially represents a small, uniform bias that is independent of drusen load (Fig 2). The small bias between the modalities is not clinically significant when compared with the effect of drusen burden on the risk of AMD progression and can be accounted for when analyzing different datasets. It should be noted that the ARA10 algorithm has been shown to have excellent repeatability on SS-OCTA scans.[10,19]

In order to understand how these differences arise, we looked at the segmentation boundaries produced by the algorithm. Figure 4 shows that the RPE segmentation follows boundaries with sharp angles differently between SS-OCTA and SD-OCTA scans, such as in the valley between the 2 large drusen at the center of the shown B-scans. A similar behavior can be seen at the margins of drusen as well (not shown). Such differences can explain the slightly larger drusen measurements found in SD-OCTA scans compared with SS-OCTA scans. Of note, no manual editing was done in this study even though such corrections can be made if desired.

It should also be noted that misidentification of the foveal center, which occurred in 4 cases, is a potential source of variability between the scan pattern results. As seen in the study by Jiang et al,[10] the algorithm can occasionally have difficulties identifying the correct foveal location on scans with large drusenoid retinal pigment epithelial detachments, such as the one shown in Figure 5. In general, measurements in the 3 mm circle are more sensitive to such misidentification than those in the 5 mm circle. Although manual corrections of the fovea location are possible, it may be preferable to routinely use the measurements within the 5 mm circle when following eyes for disease progression or recruiting patients with a defined drusen volume into clinical trials.[8,19] Overall, the ARA10 algorithm performed just as well on SD-OCTA scans as it does on SS-OCTA scans. This fact greatly enhances the clinical applicability of the ARA10 algorithm since SD-OCTA instruments are more widely used than the SS-OCTA instruments. Moreover, simple regression equations (Table 1) can be used to adjust for measurement bias when comparing drusen values obtained with the 2 different instruments. While these equations were computed using our particular sample and their general validity should be confirmed on independent samples, they are useful to compare results (based on either scan modality) presented in the literature or observed in clinical practice. It should be noted that in all situations the slope of the regression equation is not significantly different from one.

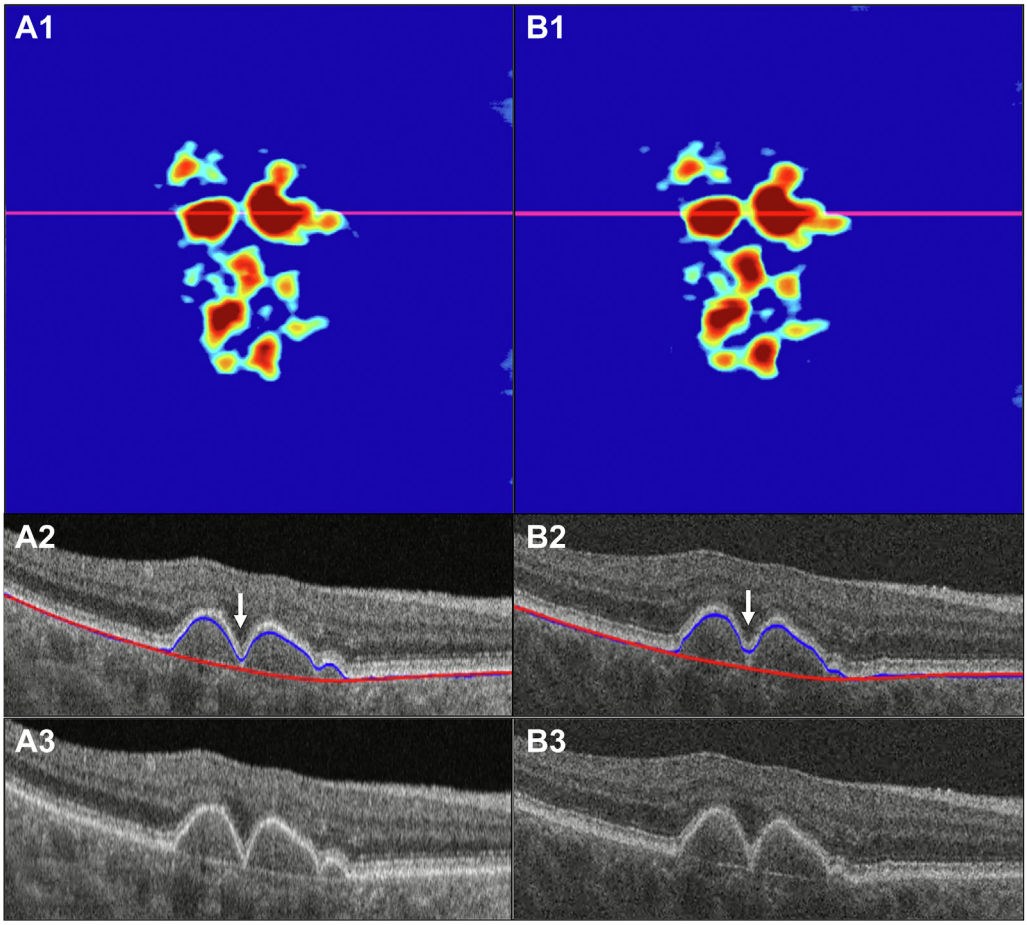


**Figure 4.** Drusen elevation maps generated by the algorithm using a swept-source OCT angiographic (SS-OCTA) scan (**A1**) and a spectral-domain OCT angiographic (SD-OCTA) scan (**B1**). **A2, A3, B2, B3,** Matched B-scans corresponding to the horizontal red lines in **A1** and **B1** are shown with, and without, segmentation lines along the retinal pigment epithelium (RPE) and Bruch's membrane (BM). **A2, B2,** The blue lines show the RPE segmentation, while the red lines show the BM segmentation. The white arrows highlight a representative difference in RPE segmentation between the SD-OCTA and SS-OCTA scans. The RPE segmentation in the SD-OCTA scan leaves a larger residual space between the RPE and BM than in the SS-OCTA scan.

The ability to use algorithms with SD-OCTA scans is an important step in our goal of using a single scan pattern for assessing disease progression in AMD. Currently, algorithms that perform drusen area and volume measurements, quantitate the total macular pigment burden, measure the outer retinal photoreceptor thickness, quantify the presence of basal laminar deposits, detect the appearance and growth of geographic atrophy, and calculate the percentage of choriocapillaris flow deficits have been introduced using the 6 mm × 6 mm SS-OCTA scan.[10,20–24] However, due to the limited clinical availability of SS-OCTA instruments, the ability to apply these algorithms to the study of AMD in multicenter clinical studies has been limited. The usefulness of these algorithms for clinical studies would increase greatly if they could be used on SD-OCTA scans. Showing that it is possible to use the ARA10 drusen algorithm on SD-OCTA scans provides a valuable step towards this goal.

While this study is limited by its small sample size, given the strength of the correlation across the wide range of drusen burdens used in the study, as well as the small mean differences reported, the inclusion of additional eyes would not be expected to change our results significantly. Another limitation is the fact that the specific algorithm we studied is proprietary and currently limited to Zeiss instruments. However, even ignoring the possibility of importing the algorithm over to other platforms, the important general conclusion is that useful structural information can be extracted from OCTA scans.

Overall, we showed that a previously validated and published algorithm for the quantitation of drusen area and volume measurements using SS-OCTA scans yielded very similar results when applied to SD-OCTA scans. The ability to use either SS-OCTA scans or SD-OCTA scans greatly broadens the clinical utility of this algorithm and provides the first demonstration of how algorithms developed for the SS-OCTA instrument can work on the more widely

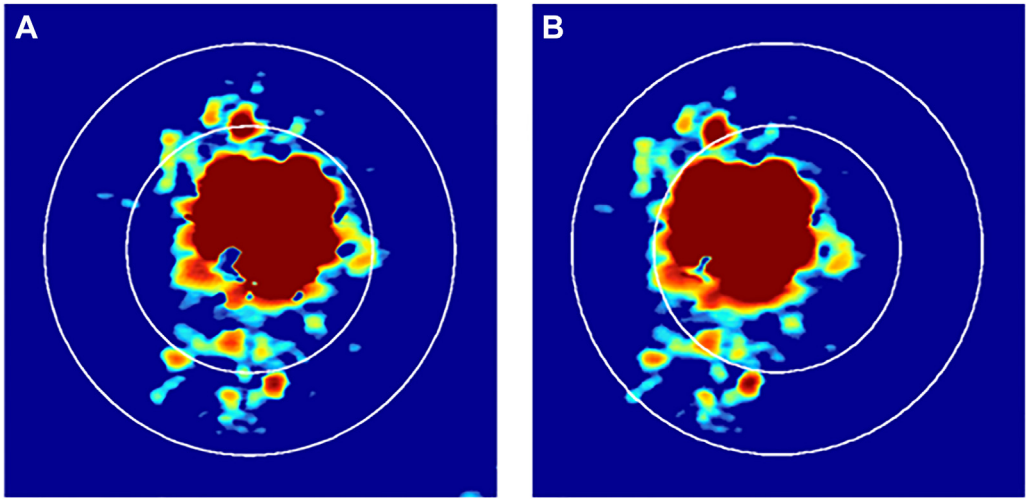


**Figure 5.** Drusen elevation maps generated by the algorithm using the spectral-domain OCT angiographic (SD-OCTA) and swept-source OCT angiographic (SS-OCTA) scans with associated 3 mm and 5 mm fovea-centered circles. **A,** The drusen elevation map generated from the SS-OCTA scan. **B,** The drusen elevation map generated from the SD-OCTA scan. As can be seen in the figure, the circles are not aligned in respect to the drusen maps displayed for each scan pattern. In this example, it was found that the fovea was correctly identified in the SD-OCTA scan. In general measurements in the 3 mm circle are more sensitive to errors due to misidentification of the fovea.

available SD-OCTA platforms. Our future aims include comparing the results of other SS-OCTA algorithms between the 2 scan modalities to provide further evidence that acquiring a single SD-OCTA scan can provide all the quantitative information typically associated with standard structural scans.

## Footnotes and Disclosures

Originally received: June 30, 2023.
Final revision: October 18, 2023.
Accepted: November 1, 2023.
Available online: November 4, 2023. Manuscript no. XOPS-D-23-00154.

[1] Department of Ophthalmology, Bascom Palmer Eye Institute, University of Miami Miller School of Medicine, Miami, Florida.

[2] Department of Ophthalmology, First Affiliated Hospital of Soochow University, Suzhou, Jiangsu, China.

[3] Research and Development, Carl Zeiss Meditec, Inc., Dublin, California.

Disclosures:

All authors have completed and submitted the ICMJE disclosures form.

The authors made the following disclosures:

Giovanni Gregori and the University of Miami co-own a patent that is licensed to Carl Zeiss Meditec, Inc.

P.H.R.: Research funding − Stealth BioTherapeutics, Gyroscope Therapeutics; Consultant − Annexon, Apellis, Bayer Pharmaceuticals, Boehringer-Ingelheim, Carl Zeiss Meditec, Genentech/Roche, Gyroscope Therapeutics, InflammX Therapeutics, Ocudyne, Regeneron Pharmaceuticals, Unity Biotechnology; Equity interest − Apellis, InflammX, Ocudyne, InflammX Therapeutics, Valitor, Inc. L.D. and Q.Z.: Employees − Carl Zeiss Meditec, Inc. The remaining authors have no disclosures.

Research supported by grants from Carl Zeiss Meditec, Inc. (Dublin, CA) (P.J.R. and G.G.), The Salah Foundation, the National Eye Institute Center Core Grant (P30EY014801), and Research to Prevent Blindness (unrestricted grant) to the Department of Ophthalmology, University of Miami, Miller School of Medicine. The sponsor or funding organization had no role in the design or conduct of this research.

HUMAN SUBJECTS: Human subjects were included in this study. The institutional review board of the University of Miami Miller School of Medicine approved the study and all patients signed an informed consent for this prospective swept-source OCT study. The study was performed in accordance with the tenets of the Declaration of Helsinki. No animal subjects were used in this study.

Author Contributions:

Conception and Design: Hiya, Shen, Zhang, Sisternes, O'Brien, Rosenfeld, Gregori

Data Collection: Hiya, Liu, Shen, Herrera, Li, Zhang, Sisternes, Rosenfeld, Gregori

Analysis and Interpretation: Hiya, Liu, Shen, Herrera, Li, Zhang, Sisternes, O'Brien, Rosenfeld, Gregori

Obtained funding: N/A

Overall Responsibility: Hiya, Liu, Shen, Herrera, Li, Zhang, Sisternes, O'Brien, Rosenfeld, Gregori

Presented at the 2023 Annual Association for Research in Vision and Ophthalmology, New Orleans, Louisiana, in April, 2023.

Abbreviations and Acronyms:
**AMD** = age-related macular degeneration; **ARA10** = Advanced RPE Analysis V0.10; **BM** = Bruch's membrane; **Cbrt** = cube root; **iAMD** = intermediate age-related macular degeneration; **RPE** = retinal pigment epithelium; **SD** = standard deviation; **SD-OCTA** = spectral-domain OCT angiography; **Sqrt** = square root; **SS-OCTA** = swept-source OCT angiography.

Keywords:
Age-related macular degeneration (AMD), Drusen, Retinal pigment epithelial (RPE) elevation, Spectral-domain OCT angiography (SD-OCTA), Swept-source OCT angiography (SS-OCTA).

Correspondence:
Giovanni Gregori, PhD, Bascom Palmer Eye Institute, 900 NW 17th Street, Miami, FL 33136. E-mail: ggregori@med.miami.edu.

## References


1. Fleckenstein M, Keenan TDL, Guymer RH, et al. Age-related macular degeneration. *Nat Rev Dis Primers*. 2021;7:31.
2. Ferris 3rd FL, Wilkinson CP, Bird A, et al. Clinical classification of age-related macular degeneration. *Ophthalmology*. 2013;120:844–851.
3. Sadda SR, Guymer R, Holz FG, et al. Consensus definition for atrophy associated with age-related macular degeneration on OCT: classification of atrophy report 3. *Ophthalmology*. 2018;125:537–548.
4. de Sisternes L, Jonna G, Greven MA, et al. Individual drusen segmentation and repeatability and reproducibility of their automated quantification in optical coherence tomography images. *Transl Vis Sci Technol*. 2017;6:12.
5. Chiu SJ, Izatt JA, O'Connell RV, et al. Validated automatic segmentation of AMD pathology including drusen and geographic atrophy in SD-OCT images. *Invest Ophthalmol Vis Sci*. 2012;53:53–61.
6. Schlanitz FG, Ahlers C, Sacu S, et al. Performance of drusen detection by spectral-domain optical coherence tomography. *Invest Ophthalmol Vis Sci*. 2010;51:6715–6721.
7. Schaal KB, Rosenfeld PJ, Gregori G, et al. Anatomic clinical trial endpoints for nonexudative age-related macular degeneration. *Ophthalmology*. 2016;123:1060–1079.
8. Sadda MGN, Humberto R-G, SriniVas R. Accuracy and reproducibility of automated drusen segmentation in eyes with non-neovascular age-related macular degeneration. *Invest Ophthalmol Vis Sci*. 2023;53:8319–8324.
9. Gregori G, Wang F, Rosenfeld PJ, et al. Spectral domain optical coherence tomography imaging of drusen in nonexudative age-related macular degeneration. *Ophthalmology*. 2011;118:1373–1379.
10. Jiang X, Shen M, Wang L, et al. Validation of a novel automated algorithm to measure drusen volume and area using swept source optical coherence tomography angiography. *Transl Vis Sci Technol*. 2021;10:11.
11. Yehoshua Z, Gregori G, Sadda SR, et al. Comparison of drusen area detected by spectral domain optical coherence tomography and color fundus imaging. *Invest Ophthalmol Vis Sci*. 2013;54:2429–2434.
12. Garcia Filho CA, Yehoshua Z, Gregori G, et al. Change in drusen volume as a novel clinical trial endpoint for the study of complement inhibition in age-related macular degeneration. *Ophthalmic Surg Lasers Imaging Retina*. 2014;45:18–31.
13. Gregori G, Yehoshua Z, Garcia Filho CA, et al. Change in drusen area over time compared using spectral-domain optical coherence tomography and color fundus imaging. *Invest Ophthalmol Vis Sci*. 2014;55:7662–7668.
14. Tan ACS, Pilgrim MG, Fearn S, et al. Calcified nodules in retinal drusen are associated with disease progression in age-related macular degeneration. *Sci Transl Med*. 2018;10:eaat4544.
15. van Leeuwen R, Klaver CC, Vingerling JR, et al. The risk and natural course of age-related maculopathy: follow-up at 6 1/2 years in the Rotterdam study. *Arch Ophthalmol*. 2003;121:519–526.
16. Yu JJ, Agron E, Clemons TE, et al. Natural history of drusenoid pigment epithelial detachment associated with age-related macular degeneration: age-related eye disease study 2 report no. 17. *Ophthalmology*. 2019;126:261–273.
17. Yehoshua Z, Wang F, Rosenfeld PJ, et al. Natural history of drusen morphology in age-related macular degeneration using spectral domain optical coherence tomography. *Ophthalmology*. 2011;118:2434–2441.
18. Schottenhamml J, Moult EM, Ploner SB, et al. OCT-OCTA segmentation: combining structural and blood flow information to segment Bruch's membrane. *Biomed Opt Express*. 2021;12:84–99.
19. Abdelfattah NS, Zhang H, Boyer DS, et al. Drusen volume as a predictor of disease progression in patients with late age-related macular degeneration in the fellow eye. *Invest Ophthalmol Vis Sci*. 2016;57:1839–1846.
20. Zhou H, Liu J, Laiginhas R, et al. Depth-resolved visualization and automated quantification of hyperreflective foci on OCT scans using optical attenuation coefficients. *Biomed Opt Express*. 2022;13:4175–4189.
21. Zhang Q, Shi Y, Shen M, et al. Does the outer retinal thickness around geographic atrophy represent another clinical biomarker for predicting growth? *Am J Ophthalmol*. 2022;244:79–87.
22. Chu Z, Shi Y, Zhou X, et al. Optical coherence tomography measurements of the retinal pigment epithelium to Bruch membrane thickness around geographic atrophy correlate with growth. *Am J Ophthalmol*. 2022;236:249–260.
23. Chu Z, Wang L, Zhou X, et al. Automatic geographic atrophy segmentation using optical attenuation in OCT scans with deep learning. *Biomed Opt Express*. 2022;13:1328–1343.
24. Chu Z, Zhang Q, Gregori G, et al. Guidelines for imaging the choriocapillaris using OCT angiography. *Am J Ophthalmol*. 2021;222:92–101.